ISSN 0020-1685, Inorganic Materials, 2019, Vol. 55, No. 7, pp. 681–686. © Pleiades Publishing, Ltd., 2019.
Russian Text © The Author(s), 2019, published in Neorganicheskie Materialy, 2019, Vol. 55, No. 7, pp. 727–732.

Thermally Controlled Formation of WO_3 Nano- and Microcrystals on the Surface of Coatings Produced on Titanium by Plasma Electrolytic Oxidation

V. S. Rudnev[a, b, *], M. S. Vasilyeva[a, b], and I. V. Lukiyanchuk[a]

[a] *Institute of Chemistry, Far East Branch, Russian Academy of Sciences, pr. Stoletiya Vladivostoka 159, Vladivostok, 690022 Russia*

[b] *Far East Federal University, ul. Sukhanova 8, Vladivostok, 690091 Russia*

**e-mail: rudnevvs@ich.dvo.ru*

Received July 31, 2018; revised January 24, 2019; accepted February 12, 2019

Abstract—We demonstrate that air annealing of oxide layers produced on titanium by plasma electrolytic oxidation and containing WO_3, $MnWO_4$, and $ZnWO_4$ leads to the surface growth of nano- and microcrystals consisting predominantly of WO_3. The crystals are initially formed around the perimeter of the coating pores. The size, composition, and number of crystals depend on the annealing temperature. We discuss possible causes and mechanisms of crystal growth.

Keywords: titanium, plasma electrolytic oxidation, surface, annealing, crystal growth

DOI: 10.1134/S0020168519070148

INTRODUCTION

There is considerable scientific and technological interest in gaining insight into general relationships underlying controlled changes in the surface architecture of oxide coatings produced on metals and alloys by plasma electrolytic oxidation (PEO). Metal/oxide layer composites produced by this method find application as protective coatings [1] and are potentially attractive as catalysts [2], for medical applications [3], and as sensing elements of sensor devices [4]. In all of these cases, an important role is played by the surface structure and composition of composite materials.

PEO is synthesis of oxide coatings on metals in electrolytes at spark and microarc discharge potentials in the electrode region [1]. Under the effect of spark and microarc discharges, oxygen-containing compounds based on electrolyte components can be formed in the composition of a growing oxide layer [5].

Tungsten oxides and transition metal tungstates have attracted research interest as photoluminescent materials [6], materials with particular magnetic characteristics [7], and catalysts [8]. PEO coatings containing stoichiometric or nonstoichiometric tungsten oxides and tungsten bronzes are commonly obtained in aqueous electrolytes containing Na_2WO_4 [9, 10] or tungsten iso- and heteropoly oxoanions [11].

As shown by Jiang et al. [12, 13], air annealing at 650–850°C of titanium samples having PEO coatings produced in a Na_3PO_4 + $Na_2B_4O_7$ + Na_2WO_4 + $M(CH_3COO)_2$ (M = Ni(II), Zn(II), Mn(II)) electrolyte and then impregnated with nickel(II) nitrate or Zn(II) nitrate solutions or without additional impregnation in the case of Mn(II) leads to the formation of nanorods, nanogrids, nanoflowers, nanostrips, or nanowhiskers from $NiWO_4$, $ZnWO_4$, or $MnWO_4$, respectively. According to Jiang et al. [12, 13], these tungstates in an amorphous state are present even in the initial PEO coating and act as nuclei for the growth of nanostructures at elevated temperatures. Electrolyte or impregnation solution components accumulating in pores of coatings can serve as sources for the growth of nanoparticles.

Similarly, 850°C annealing of PEO coatings produced on titanium in an electrolyte containing $Ce_2(SO_4)_3$ + $Zr(SO_4)_2$ leads to the formation of rutile TiO_2 nano- and microcrystals on their surface [14]. Note that the nanocrystals first grow in or near pores. The formation of crystals was tentatively attributed to high-temperature titanium diffusion from the bulk along pore walls to the surface and titanium oxidation resulting in the formation of crystals of the rutile phase, corresponding to this temperature. Prolonged annealing increases the crystal size, and the entire surface becomes covered with crystals.

There is conclusive evidence [12–14] that air annealing of PEO layers with a complex oxide composition is a promising approach for the thermally stimulated growth of nano- and microstructures of partic-

Table 1. Compositions of the electrolytes and designations of the samples

Electrolyte composition	Designations of the samples
Basic: 0.1 M Na_2WO_4 + 0.84 M CH_3COOH + 0.01 M NaOH	Ti/W
Basic + 0.04 M $Mn(CH_3COO)_2$	Ti/W,Mn
Basic + 0.04 M $Zn(CH_3COO)_2$	Ti/W,Zn

ular composition and geometry attached to their surface.

In this paper, we examine the effect of annealing on the transformation of the surface composition and architecture of PEO coatings produced on titanium in Na_2WO_4-based electrolyte.

EXPERIMENTAL

Electrodes in the form of plates 2.0 × 2.0 cm in dimensions were produced from VT1-0 titanium sheet. To remove the surface layer of the metal and standardize the surface, the samples were chemically polished in a 1 : 3 mixture of concentrated HF and HNO_3 at 60–80°C for 2–3 s.

Electrolytes were prepared using commercially available chemicals: $Na_2WO_4 \cdot 2H_2O$ (analytical grade), glacial CH_3COOH (reagent grade), NaOH (analytical grade), $Mn(CH_3COO)_2 \cdot 4H_2O$ (analytical grade), $Zn(CH_3COO)_2 \cdot 2H_2O$ (analytical grade), and distilled water. The compositions of the electrolytes used and the designations of the samples obtained in them are indicated in Table 1.

Coatings were produced using a TER4-100/460N thyristor converter operated in pulsed unipolar mode. Oxide films on titanium were formed in galvanostatic mode at an effective current density $i = 0.2$ A/cm^2. The process was carried out for 10 min in a 1-L heat-resistant glass vessel. The cathode had the form of stainless steel pipe coil cooled by tap water. The initial electrolyte temperature was 14–23°C. After PEO, the samples were washed with water and dried in air at room temperature.

Next, the samples were calcined in a muffle furnace in air for 1 h at temperatures of 700 or 850°C.

The phase composition of the samples was determined by X-ray diffraction (XRD) on a D8 ADVANCE diffractometer (Germany) with CuK_α radiation by a standard procedure. The compounds present in the samples were identified in automatic mode using EVA search software and ICDD PDF-2 data.

To determine the elemental composition of the coatings and examine their surface microstructure, we used a Hitachi S-5500 scanning electron microscope (SEM) (Japan) equipped with an energy dispersive X-ray microanalysis system. The depth of the analyzed layer was ~1 μm.

RESULTS AND DISCUSSION

Figure 1 shows an unannealed coating surface (Fig. 1a) and coating surfaces after annealing at 700 (Figs. 1b, 1c, 1e) or 850°C (Figs. 1d, 1f). In all cases examined, after annealing at a temperature of 700°C we observed chains of regularly shaped crystals formed around the perimeter of the pores (Figs. 1b, 1c, 1e). Annealing at 850°C led to the formation of markedly larger crystals (Figs. 1d, 1f). Moreover, annealing at 850°C led to changes in surface structure over most of the coating. Both before (Fig. 1a) and after annealing at 700°C (Figs. 1b, 1c, 1e), the surface layer was dense and appeared uniform at the magnification used, but annealing at 850°C converted it into an array of grain-like nanoparticles (Figs. 1d, 1f).

Changes in the architecture of the surface and the formation of crystalline nano- and microstructures on it are well consistent with XRD data. The unannealed Ti/W coatings were poorly crystallized (Fig. 2a). In addition to an amorphous halo, there were relatively weak reflections from WO_3, $Na_{0.28}WO_3$ tungsten bronze, and anatase TiO_2. After annealing at 700 and 850°C, the coatings contained well-defined crystalline tungsten oxide phases (Figs. 2b, 2c). After annealing at 850°C, XRD characterization showed that the coatings contained no tungsten bronze and that titanium oxide was present in the form of rutile, a high-temperature phase.

Annealing the Ti/W,Mn and Ti/W,Zn coatings produced in electrolytes containing manganese(II) or zinc(II) acetates generally leads to similar changes in the surface structure and composition of the coatings (Figs. 1e, 1f, 2d–2f). The main distinctions are a more complex surface morphology over most of the coating after annealing at 850°C (cf. Figs. 1d and 1f) and the presence of reflections from crystalline $MnWO_4$ and $ZnWO_4$ in the XRD patterns of the annealed coatings. Note also weak reflections from these phases in the XRD patterns of the unannealed coatings (Fig. 2d).

Table 2 presents the average compositions of the coatings and the crystals formed. Calculations using the data obtained in this study suggest that the composition of the annealed materials corresponds to the presence of TiO_2 and WO_3 in the Ti/W samples; TiO_2, WO_3, and $MnWO_4$ in the Ti/W,Mn samples; and TiO_2, WO_3, and $ZnWO_4$ in the Ti/W,Zn samples. Thus, the elemental compositions of the coatings are consistent with the XRD data (Fig. 2). The presence of carbon in some cases may be due either to its incorpo-

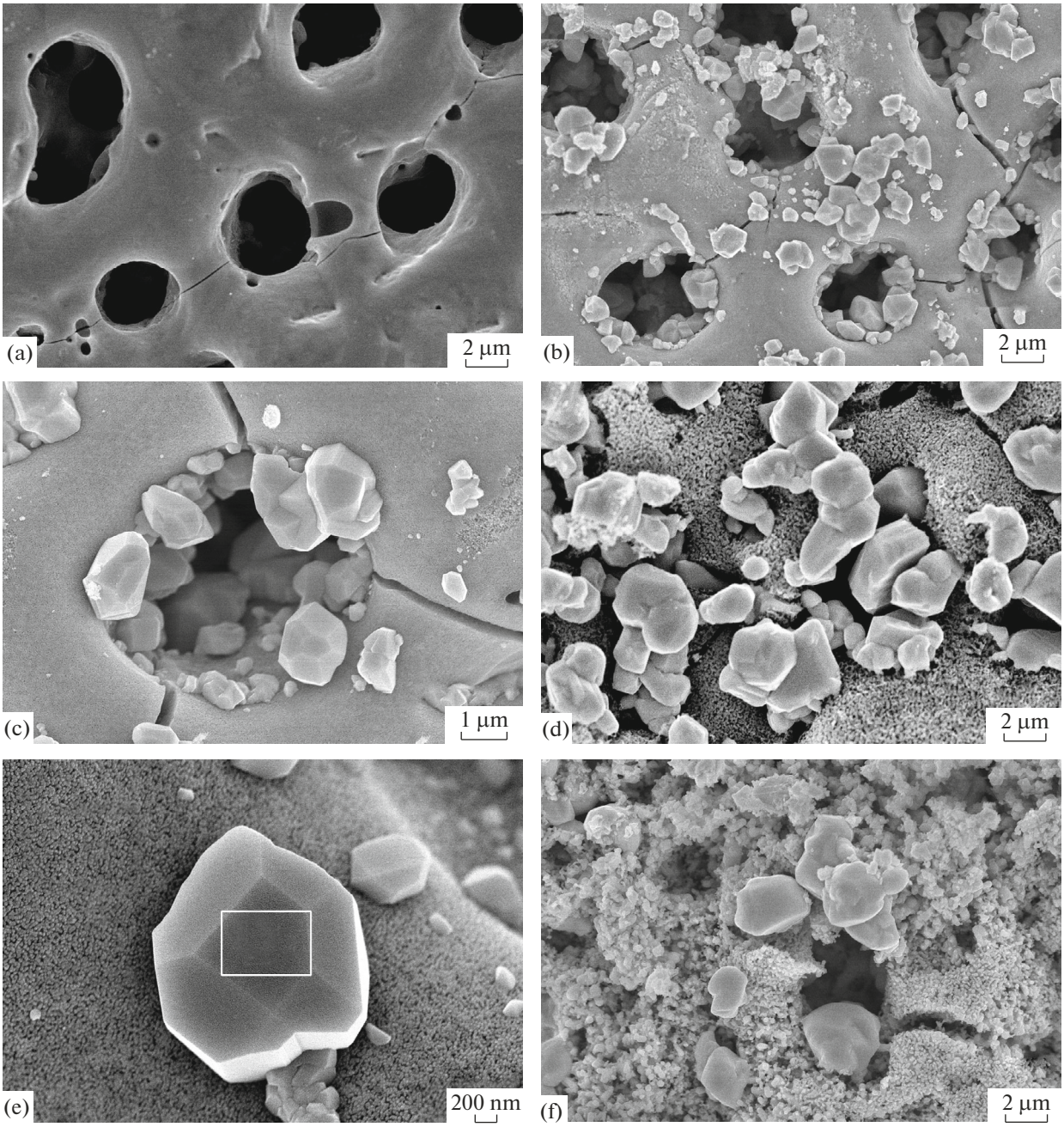

Fig. 1. SEM images of the surface of the (a–d) Ti/W, (e) Ti/W,Zn, and (f) Ti/W,Mn samples: unannealed (a) and annealed at 700 (b, c, e) and 850°C (d, f).

ration from the electrolyte during PEO or to the contamination of samples during handling.

The crystals formed during annealing at 700°C consist predominantly of tungsten and oxygen, but the percentage of oxygen is insufficient for the formation of the stoichiometric oxide WO_3. The elemental analysis data lead us to assume that the crystals consist of WO_3 + ?W (Table 2). After annealing at 850°C, the crystals contain titanium as an additional phase, so we assume their composition to be $WO_3 + TiO_2 + ?W + ?Ti$.

Thus, annealing the coatings at temperatures above 700°C leads to the formation of tungsten oxide-containing nano- and microcrystals on their surface. The annealed Ti/W,Mn and Ti/W,Zn coatings typically contain crystalline $MnWO_4$ and $ZnWO_4$, respectively. At the same time, unlike Jiang et al. [12, 13] we did not detect growth of crystalline nanostructures containing such phases on the surface. According to Jiang et al. [12, 13], assumed necessary conditions for the growth of $MnWO_4$ and $ZnWO_4$ nanocrystals are the presence

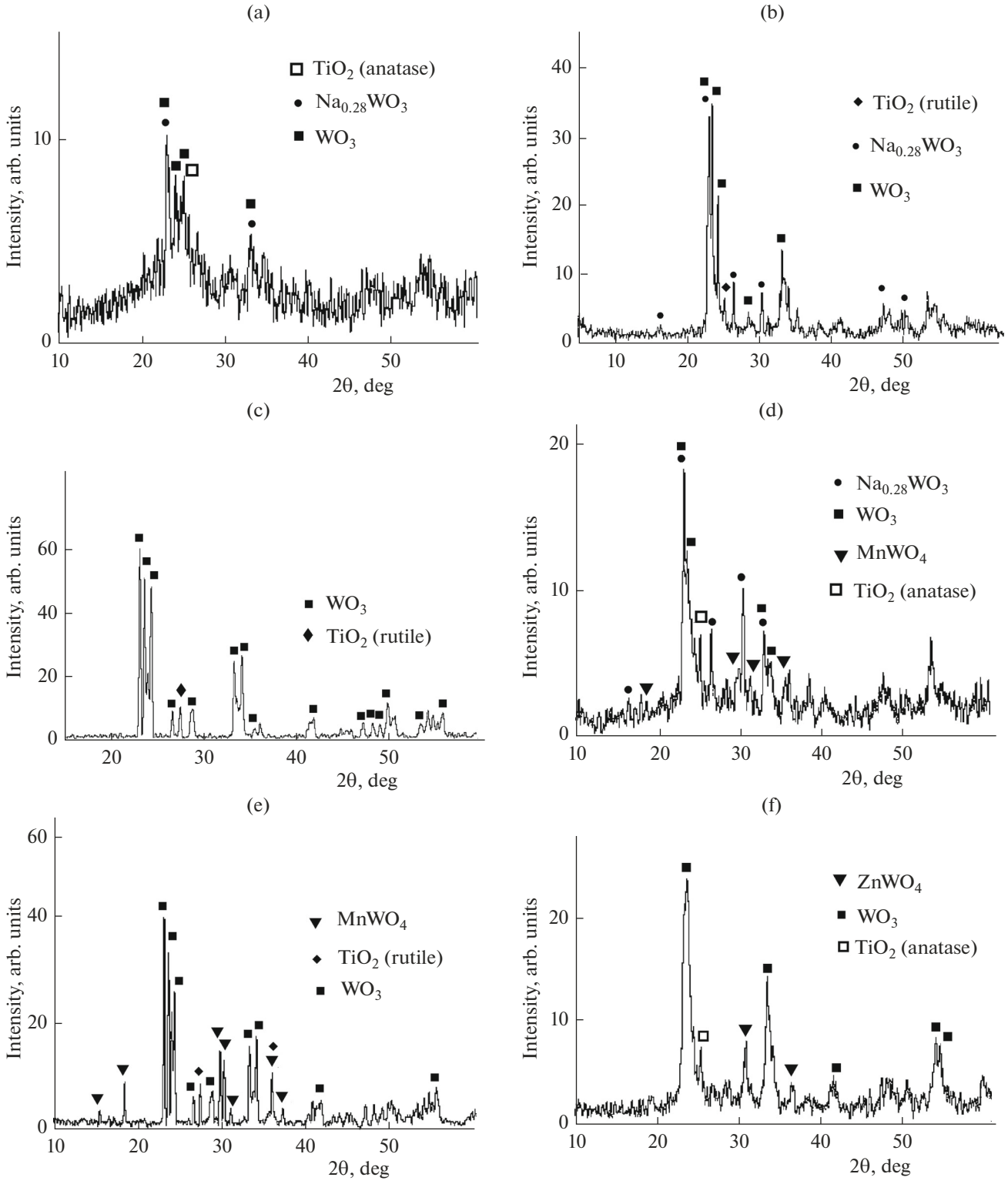

Fig. 2. X-ray diffraction patterns of the (a–c) Ti/W, (d, e) Ti/W,Mn, and (f) Ti/W,Zn samples: unannealed (a, d) and annealed at 700 (b, f) and 850°C (c, e).

of crystalline nuclei of these phases in the composition of the coatings and the delivery of components for their growth from the electrolyte salts or the impregnation solution in the pores of the coatings. It seems likely that the distinction can be accounted for in terms of the qualitative and quantitative compositions

Table 2. Elemental composition (at %) and calculated phase composition of the coatings and the crystals formed

Sample	Composition			
	700°C		850°C	
	coating	crystal	coating	crystal
Ti/W	O 70.3; Ti 14.7; W 14.9 ($WO_3 + TiO_2$)	O 62.5; W 37.5 (WO_3 + ?W)	O 70.3; Ti 19.2; W 10.5 ($WO_3 + TiO_2$)	O 67.7; Ti 12.2; W 20.1 ($WO_3 + TiO_2$ + ?W + ?Ti)
Ti/W,Mn	C 7.2; O 64.0; Ti 3.4; W 16.7; Mn 6.8 ($WO_3 + TiO_2 + MnWO_4$)	C 11.4; O 66.0; W 23.2; Mn 1.2 (WO_3 + ?W)	C 5.4; O 62.4; Ti 15.9; W 9.7; Mn 6.6 ($WO_3 + TiO_2 + MnWO_4$)	C 7.8; O 58.5; Ti 5.9; W 30.1; Mn 0.6 ($WO_3 + TiO_2$ + ?W + ?Ti)
Ti/W,Zn	C 23.0; O 63.0; Ti 10.0; W 14.0; Zn 3.0 ($WO_3 + TiO_2 + ZnWO_4$)	O 52.2; W 47.8 (WO_3 + ?W)	No data	No data

"Coating" here means areas 100 × 75 μm in dimensions; "crystal" means areas on crystals (Fig. 1e), in both cases average over three to five areas. In parentheses, we give a tentative phase composition of the coatings and crystals inferred from their elemental compositions.

of the electrolytes for PEO, including the increased sodium tungstate concentration in this study and the reduced metal(II) acetate concentrations in comparison with the solutions used by Jiang et al. [12, 13].

As mentioned above, after annealing, the WO_3 nano- and microcrystals are initially located around pore perimeters and along cracks in the bulk of the coatings (Figs. 1b–1d). The pore in Fig. 1c is seen to also contain crystals. It seems likely that crystals begin to grow in pores and that, as their size increases, the growing crystals become forced out to the surface and propagate over it. The described observation is consistent with the assumption made by Jiang et al. [12, 13] as to the role that the residual electrolyte in the pores plays in the formation of nano- and microcrystals during annealing. On the other hand, as shown earlier [14] annealing in air at a temperature of 850°C produces TiO_2 nano- and microcrystals on the surface of PEO coatings produced on titanium in a $Ce_2(SO_4)_3$ + $Zr(SO_4)_2$ electrolyte. Like in this study, the crystals first appear near pores and then cover the entire surface. The tentative mechanism behind this effect is the high-temperature oxidation of the main metal in the coating through oxygen diffusion, titanium counterdiffusion along pore walls to the surface, and the growth and displacement of TiO_2 crystals to the surface. Most likely, both processes are responsible for the formation of WO_3 crystals on the surface in this study. For example, annealing at a temperature of 700°C produces WO_3 crystals in pores of the coatings due to the residual electrolyte components, predominantly Na_2WO_4 in our case. The crystals grow and some of them become forced out to the surface. As the annealing temperature is raised to 850°C, TiO_2 crystals begin to form deep in pores. As a result of this process, the WO_3 crystals more rapidly leave the pores and the TiO_2 crystals more readily reach the surface. This is evidenced, albeit indirectly, by the presence of titanium in the composition of the crystals on the surface (Table 2).

In addition, in a number of publications, reduced metals present in both the electrolyte and the material being processed were reported to be located in craters and pores of coatings [15–17]. It also cannot be ruled out that crystals are formed in pores as a result of the high-temperature oxidation of these metals and then reach the surface.

It seems likely that all of the above-mentioned factors contribute to the thermally stimulated formation of nano- and microcrystals and their propagation over the surface of PEO coatings. Further research is needed to gain insight into the mechanism of crystal growth on the surface of PEO coatings and assess the feasibility of controlling their composition, size, and shape.

CONCLUSIONS

Annealing at temperatures above 700°C leads to the formation of WO_3 nano- and microcrystals of regular geometric shape on the surface of PEO coatings produced on titanium in sodium tungstate-based electrolytes. The size and number of crystals grow with increasing annealing temperature. Crystals begin to form around pore perimeters and then propagate over the coating surface. The addition of manganese(II) and zinc(II) acetates to an electrolyte leads to the formation of crystalline $MnWO_4$ and $ZnWO_4$ in the bulk of the coatings.

The results obtained in this study, in combination with previously reported data, demonstrate that annealing in air at temperatures above 700°C can be used to produce ensembles of attached nano- and microcrystals of particular composition on the surface of PEO coatings with a complex oxide composition on titanium.

FUNDING

This work was supported by the Russian Foundation for Basic Research, grant no. 18-03-00418.

REFERENCES

1. Suminov, I.V., Belkin, P.N., Epel'fel'd, A.V., Lyudin, V.B., Krit, B.L., and Borisov, A.M., *Plazmenno-elektroliticheskoe modifitsirovanie poverkhnosti metallov i splavov* (Plasma Electrolytic Surface Modification of Metals and Alloys), Moscow: Tekhnosfera, 2011.
2. Patcas, F. and Krysmann, W., Efficient catalysts with controlled porous structure obtained by anodic oxidation under spark-discharge, *Appl. Catal. A-Gen.,* 2007, vol. 316, no. 2, pp. 240–249. https://doi.org/10.1016/j.apcata.2006.09.028
3. Rokosz, K., Hryniewicz, T., and Raaen, S., Development of plasma electrolytic oxidation for improved Ti_6Al_4V biomaterial surface properties, *Int. J. Adv. Manuf. Technol.,* 2016, vol. 85, pp. 2425–2437. https://doi.org/10.1007/s00170-015-8086-y
4. Marinina, G.I., Vasilyeva, M.S., Lapina, A.S., Ustinov, A.Yu., and Rudnev, V.S., Electroanalytical properties of metal-oxide electrodes formed by plasma electrolytic oxidation, *J. Electroanal. Chem.*, 2013, vol. 689, pp. 262–268. https://doi.org/10.1016/j.jelechem.2012.10.032
5. Gordienko, P.S., *Obrazovanie pokrytii na anodno-polyarizovannykh elektrodakh v vodnykh elektrolitakh pri potentsialakh iskreniya i proboya* (Growth of Coatings on Anodically Polarized Electrodes in Aqueous Electrolytes at Spark and Breakdown Voltages), Vladivostok: Dal'nauka, 1996.
6. Cho, H.D., Yoon, I.T., Chung, K.B., Kim, D.Y., Kang, T.W., and Yuldashev, Sh.U., Low-temperature photoluminescence of WO_3 nanoparticles, *J. Lumin.,* 2018, vol. 195, pp. 344–347. https://doi.org/10.1016/j.jlumin.2017.11.053
7. Zhou, Y.-X., Yao, H.-B., Zhang, Q., Gong, J.-Y., Liu, S.-J., and Yu, S.-H., Hierarchical $FeWO_4$ microcrystals: solvothermal synthesis and their photocatalytic and magnetic properties, *Inorg. Chem.,* 2009, vol. 48, pp. 1082–1090. https://doi.org/10.1021/ic801806r
8. Zhang, C.L., Zhang, H.L., Zhang, K.Y., Li, X.Y., Leng, Q., and Hu, C.G., Photocatalytic activity of $ZnWO_4$: band structure, morphology and surface modification, *ACS Appl. Mater. Interfaces,* 2014, vol. 6, pp. 14 423–14 432. https://doi.org/10.1021/am503696b
9. Gruss, L.L. and McNeil, W., Anodic spark reaction product in aluminate, tungstate and silicate solutions, *Electrochem. Technol.,* 1963, vol. 1, nos. 9–10, pp. 283–287.
10. He, J., Luo, Q., Cai, Q.Z., Li, X.W., and Zhang, D.Q., Microstructure and photocatalytic properties of WO_3/TiO_2 composite films by plasma electrolytic oxidation, *Mater. Chem. Phys.,* 2011, vol. 129, pp. 242–248. https://doi.org/10.1016/j.matchemphys.2011.04.011
11. Lukiyanchuk, I.V., Rudnev, V.S., Tyrina, L.M., Panin, E.S., and Gordienko, P.S., Anodic-spark layers formed on aluminum alloy in tungstate–borate electrolytes, *Russ. J. Appl. Chem.,* 2002, vol. 75, no. 12, pp. 1972–1978. https://doi.org/10.1023/A:1023395616974
12. Jiang, Y.N., Liu, B., Zhai, Z., Liu, X., Yang, B., Liu, L., and Jiang, X., A general strategy toward the rational synthesis of metal tungstate nanostructures using plasma electrolytic oxidation method, *Appl. Surf. Sci.,* 2015, vol. 356, pp. 273–281. https://doi.org/10.1016/j.apsusc.2015.08.080
13. Jiang, Y.N., Liu, B.D., Yang, W.J., Yang, B., Liu, X.Y., Zhang, X.L., Mohsin, M.A., and Jiang, X., New strategy to the in-situ synthesis of single-crystalline $MnWO_4/TiO_2$ photocatalysts for efficient and cyclic photodegradation of organic pollutant, *CrystEngComm,* 2016, vol. 18, pp. 1832–1841. https://doi.org/10.1039/c5ce02445e
14. Vasilyeva, M.S., Rudnev, V.S., Wiedenmann, F., Wybomov, S., Yarovaya, T.P., and Jiang, X., Thermal behavior and catalytic activity in naphthalene destruction of Ce-, Zr- and Mn-containing oxide layers on titanium, *Appl. Surf. Sci.,* 2011, vol. 258, no. 2, pp. 719–726. https://doi.org/10.1016/j.apsusc.2011.07.127
15. Rudnev, V.S., Lukiyanchuk, I.V., Adigamova, M.V., Morozova, V.P., and Tkachenko, I.A., The effect of nanocrystallites in the pores of PEO coatings on their magnetic properties, *Surf. Coat. Technol.,* 2015, vol. 269, no. 1, pp. 23–29. https://doi.org/10.1016/j.surfcoat.2015.01.073
16. Rakoch, A.G., Magurova, Yu.V., Bardin, I.V., El'khag, G.M., Zharinov, P.M., and Kovalev, V.L., Exothermal oxidation of the bottom of discharge channels upon microarc oxidation of aluminum alloys, *Prot. Met. Phys. Chem. Surf.,* 2008, vol. 44, no. 7, pp. 710–714. https://doi.org/10.1134/S0033173208070114
17. Rogov, A.B., Terleeva, O.P., Mironov, I.V., and Slonova, A.I., Iron-containing coatings obtained by microplasma method on aluminum with usage of homogeneous electrolytes, *Appl. Surf. Sci.,* 2012, vol. 258, no. 7, pp. 2761–2765. https://doi.org/10.1016/j.apsusc.2011.10.128